

Scaling Ergodic Control for Large-Scale Problems: Intra-Forest Exploration with a Moving Gaussian Mixture Model

Adam Seewald¹, Ian Abraham², and Stefano Mintchev¹

Abstract—

I. INTRODUCTION

Exploring unknown and potentially large-scale spaces with robots is a problem commonly addressed by different methodologies arising in computing and robotics. This problem is recurring in real-world use case such as monitoring, reconstruction, exploration, etc., where robots are expected to cover a given space while performing an assigned task. A key challenge to the practical applicability of these methodologies is that of leveraging resources, while, at the same time, maximizing the information gathered and optimizing the exploration accordingly [1, 2]. While there are different approaches in the literature, approaches that are informed by sensory data have emerged as of particular interest. Among these approaches, ergodic control is a significant result, as it provides a more natural way of searching through deterministic exploratory behaviours while accounting for both the motion cost and optimality [3].

Ergodic control is a planning and controls methodology that derives robot trajectories maximizing a given information measure, so that robots spend more time in areas with high information measure while quickly traversing areas with low information measure [4–6]. As a consequence, it is required that the user provides an information measure a priori, or that, the information measure is derived as the robots gather more information about their surroundings. While applicable to some use cases, this is often a limitation of the existing ergodic controllers. It is indeed not always the case the information measure can be easily refined from the gathered data, or, that an a-priori information measure can be provided at all. With this work we addressed this challenge. We provide a general and scaled ergodic control methodology that can be applied to a broader class of robotic use cases at large-scale. Our methodology does not require an underlying information measure but rather derives an information measure from the exploration itself, and refines such measure utilizing information about already visited areas and obstacles from sensory data. Furthermore, conversely to existing ergodic control methodologies that require external obstacle avoidance techniques, e.g., control barrier functions [7], optical flow [8], etc., our methodology provides a tunable degree of obstacle avoidance as a “by-product.” The underlying information measure is represented

utilizing a Gaussian Mixture Model (GMM), which is refined – a process that is handled by our methodology and that does not require any user input – from the sensory data as the robot traverses the state space. Our ergodic formulation is different from existing methods. The problem is posed so that the robot spends time in areas with low information measure, whereas the “explored space” is related to high information measure. The methodology is iterative and utilizes a model predictive controller (MPC) approach, where the ergodic controller is refined within a specified time window.

Existing ergodic controllers have been studied from the point of view of time [9] and energy [10, 11] optimality and applied to a multitude of use cases. These use cases include tactile sensing [5], active learning [12], multi-objective optimality [13, 14], grasping and manipulation [15, 16] and visual rendering [17, 18]. Ergodic controllers in the literature feature diverse aspects such as stochastic dynamics [19, 20] and multi-agent and/or swarm control with both centralized [10, 21] and distributed information processing [8, 22]. Although some of these use-cases involve information gathering [23] and features urban environments and other potentially large-scale problems [8, 24], a generic large-scale ergodic controller has not been studied yet. Even though recent methods have been making progress in this direction [9–11, 25], these methods do not scale efficiently due to the formulation of the underlying optimization and/or require an a-priori information measure. From an obstacle avoidance perspective, even though there are ergodic controllers that feature obstacle avoidance [7], this is an external component on top of the ergodic controller that then results in a sub-ergodic solution [9], rather than an integral component of the explorer itself.

We show case our general and scaled ergodic control on a large-scale problem: the problem of exploring a forest or a densely vegetated area, in contrast to existing ergodic control methodologies that are demonstrated in structured environments, in simulation, or generally in small-scale only. Section IV shows the performance of our methods with both simulated and real-world data. The open-source software stack to replicate our approach is made available on our project repository webpage¹.

The remainder of this paper is then structured as follows. Sec. II provides the details of the underlying principles and the problem addressed. Sec. III is split into two sub-sections, one provides an overview of ergodic control whereas the other one details our methodology. Sec. V provides conclusions and draws future perspectives.

This work was partly supported by ETH Zürich’s World Food System Center and Yale University.

¹A.S. and S.M. are with the Department of Environmental Systems Science, ETH Zürich, Switzerland. Email: aseewald@ethz.ch;

²I.A. is with the Department of Mechanical Engineering and Materials Science, Yale University, CT, USA.

II. PROBLEM FORMULATION

This work addresses the problem of exploring a bounded and potentially large-scale space, whereby large-scale we indicate spaces of orders of dozens or even hundred of meters in both x- and y-axis. For practical reasons, we bound the exploration space, i.e., the space to be explored, to one hectare, and we consider the exploration in two-dimensions. The formulation is such, however, that the state space might be potentially unbounded, and not limited to two dimensions [9].

Let us thus consider such bounded space $\mathcal{Q} \subset \mathbb{R}^2$. The robot is free to move in the space except for a finite number of obstacles represented by $\mathcal{O} \subset \mathcal{Q}$. In the remainder, we utilize the concepts of ergodicity and ergodic metric to direct the robot into unexplored areas while avoiding the obstacles, i.e., $\mathcal{Q} \cap \mathcal{O}$, as opposed to other works on ergodic control in the literature where the exploration happens in areas of high information density instead [4–6].

Definition II.1 (Ergodicity). Given the bounded state space \mathcal{Q} , a trajectory $\mathbf{x}(t) \in \mathcal{Q}$ is *ergodic* w.r.t. a spatial distribution ϕ , or, analogously, is distributed among regions of high expected distribution, if and only if

$$\lim_{t \rightarrow \infty} \int_{\mathcal{Q}} \phi(\mathbf{x}) \Omega(\mathbf{x}) d\mathbf{x} = \frac{1}{t} \int_{\mathcal{T}} \Omega(\bar{\mathbf{x}}(t)) dt, \quad (1)$$

where $\bar{\cdot}$ is a map that maps the state space to the exploration spaces, and Ω are all the Lebesgue function as defined in, e.g., [?].

The spatial distribution ϕ is built utilizing a Gaussian Mixture Model (GMM).

Definition II.2 (Moving GMM). Assume that there is a given number $n \in \mathbb{N}_{>0}$ of Gaussians \mathcal{N} in a GMM, whose initial probability is equally distributed. A *moving GMM* is

$$\phi(\boldsymbol{\alpha}, \boldsymbol{\mu}, \mathbf{x}) := \sum_{i=1}^n \alpha_i \mathcal{N}_i(\mathbf{x} | \mu_i, \Sigma_i), \quad (2)$$

where $\Sigma_i \in \mathbb{R}^{2 \times 2}$ indicates the the covariance matrix and $\mu_i \in \mathcal{Q}$ the center of a Gaussian \mathcal{N}_i , i.e., a GMM with variable centers $\boldsymbol{\mu} \in \mathcal{Q}^n$ and mixing coefficients $\boldsymbol{\alpha} \in \mathbb{R}_{>0}^n$.

Bold letters indicate vector, i.e., $\mathbf{x} \in \mathcal{Q}$ is the state space vector whereas $\boldsymbol{\alpha}, \boldsymbol{\mu}$ are the vectors compromising ideal GMM's probability and position components respectively (see Section III).

An ergodic metric is a value that quantifies the ergodicity.

Definition II.3 (Ergodic metric). Consider a time average distribution of the trajectory over a limited time window t , e.g.,

$$h(\mathbf{x}(t)) := \frac{1}{t} \int_{\mathcal{T}} \Delta((\mathbf{x})(t)) dt. \quad (3)$$

Δ is defined as a Dirac delta function. An *ergodic metric* is an L^2 -inner product in between the average of the spatial and time distributions.

Problem II.1 (Scaled ergodic control). Given the state space and the obstacles space \mathcal{Q} and \mathcal{O} respectively, assume the number of components n of a GMM is given. The *scaled*

ergodic control problem is the problem of finding the evolution of the components of the moving GMM, i.e., $\alpha(t)$ and $\mu(t)$ and of the control $\mathbf{u}(t) \in \mathcal{U}$ so that $\mathbf{x}(t)$ explores \mathcal{Q} while avoiding \mathcal{O} and, the ergodic metric is minimized.

We propose a solution to Problem II.1 and demonstrate both by simulation and real-world experiment the feasibility of the solution, underlying the existence of trade-offs in between the accuracy and the exploration soundness in Sec. IV and IV respectively.

III. METHODS

This section details our methods. Sec. III-A introduces the concept of canonical ergodic control for exploration in bounded areas with an information density distribution. Sec. III-B describes our methodology of scaled ergodic control, i.e., ergodic control with a moving information density as a function of explored against unexplored space.

A. Canonical ergodic control

To quantify the time average and the average of the spatial distributions h and ϕ respectively, let us consider Fourier series basis functions [?]. For the time average distribution, the coefficients of an equivalent basis function can be expressed

$$c_k(\mathbf{x}(t)) := \int_{\mathcal{T}} \prod_{d \in \{1,2\}} \cos(2\pi k_d \mathbf{x}_d(\tau)/T) / T^2 d\tau / t, \quad (4)$$

where $T \in \mathbb{R}_{>0}$ is a given period. \cdot_d indicates the d th item of a vector.

Equation (4) expresses the cosine basis function for a coefficient k , i.e., we consider only the positive slice of the spectral domain and thus ignore the function's imaginary component. The coefficients $k \in \mathcal{K}$ depend on a given number of frequencies $\kappa \in \mathbb{N}_{>0}$ and are built so that $\mathcal{K} \in \mathbb{N}^2$ is a set of index vectors that cover the set $\kappa \times \dots \times \kappa \in \mathbb{N}^{\kappa^2}$, i.e., the coefficients are evaluated on the entire domain.

For the average of the spatial distribution, the coefficients of an equivalent basis function can be expressed similarly

$$\phi_k(\mathbf{x}) := \int_{\mathcal{Q}} \sum_{d \in \{1,2\}} \phi(\mathbf{x}) c(\mathbf{x}) d\mathbf{x}, \quad (5)$$

where c is the integrand in Eq. (4) in the given point \mathbf{x} at the current time step.

The aim of an ergodic controller is to minimize an ergodic metric, i.e., the L^2 -inner product of the distributions h and ϕ (see Definition II.3). A consolidated metric [5, 7, 9, 10, 12, 26] for this purpose is, for instance

$$\mathcal{E}(\mathbf{x}) := \sum_{k \in \mathcal{K}} \Lambda_k (c_k - \phi_k)^2 / 2, \quad (6)$$

where the coefficients of the time average and the average spatial distributions are expressed in Eq. (4–5). Λ_k is a weight factor that expresses which frequency has more weight, e.g., with

$$\Lambda_k := \frac{1}{\sqrt{(1 + \|k\|^2)^3}}, \quad (7)$$

lower frequencies are to be preferred.

Note that in Eq. (5) we have utilized the expression for a standard GMM. We utilize the expression of the moving GMM in the next section.

B. Scaled ergodic control

To utilize the concept of moving information density as a function of explored against unexplored space, let us first consider Eq. (5) with the moving GMM from Definition II.2.

Let us assume for practical purposes that the space is square, with a given length $l \in \mathbb{R}_{>0}$ expressed in meters. Let us thus tight the period in Eq. (4) to such search space and express $l = T/2$. Eq. 5 can be expressed

$$\phi_k(\alpha, \mu, \mathbf{x}) := \int_{\mathcal{Q}} \left(\sum_{d \in \{1,2\}} \sum_{i=1}^n \alpha_i \mathcal{N}_i(\mathbf{x} | \bar{\mu}_i, \bar{\Sigma}_i) \right) c(\mathbf{x}) d\mathbf{x}, \quad (8)$$

where $\bar{\cdot}$ is map that maps the center and the covariance matrix to a symmetric state space delimited by $-l$ and l by, e.g., using linear transformation matrices [27].

Let us further define a given value that expresses the concept of “history.” If this value is expressed by, $h \in \mathbb{R}_{>0}$, we can model the concept of the “already explored space” exploiting the definition of the moving GMM. The covariance matrix can be expressed

$$\Sigma_i := \frac{1}{2T} \int_{\Upsilon} \sum_{d \in \{1,2\}} (\mathbf{x}_d(\tau) - \mu_i) d\tau, \quad (9)$$

where the trajectory is being evaluated within the history, i.e., Υ indicates the time interval in between t and $t - h$. The centers can be then expressed as $\mu_i := E(\mathbf{x}(t))$ with E being the expected value of \mathbf{x} on Υ .

The scaled ergodic control problem can then be expressed as the problem of finding an ergodic controller that visit the inverse of the probability distribution represented by the moving GMM, thus avoiding areas “already visited,” within a given history window h . The problem posed in this way, however, produces trajectories that require an additional obstacle avoidance methodology, such as [7].

Let us thus consider a modified expression for the center of the gaussian $\mu_i := E(\mathbf{x}(t)) - \mathbf{e}_i$ where $\mathbf{e}_i \in \mathbf{e} \subset \mathbb{R}^n$ is a displacement that allow to “move” the Gaussian components in the moving GMM.

Our methodology is such that the scaled ergodic controller finds the minimum displacement of the Gaussians so that the the space to be visited is delimited by $\mathcal{Q} \cap \mathcal{O}$. Such controller can be expressed with the optimal control problem (OCP)

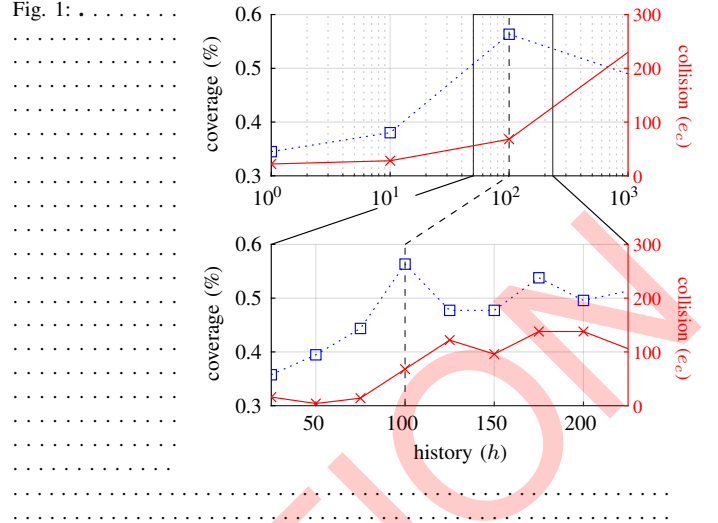
$$\min_{\Theta} \mathcal{E}(\mathbf{x}) + \Psi(\mathbf{e}), \quad (10a)$$

$$\text{s.t. } \dot{\mathbf{x}} = f(\mathbf{x}(t), \mathbf{u}(t)), \quad (10b)$$

$$\mathbf{x}(t) \in \mathcal{Q} \cap \mathcal{O}, \mathbf{u}(t) \in \mathcal{U}, \quad (10c)$$

$$\mathbf{x}(t_0), n, \kappa, l, h, \text{ are given}, \quad (10d)$$

where the output of the optimization Θ in Eq. (10a) is $\mathbf{x}, \mathbf{u}, \alpha, \mu$, i.e., the center of each Gaussian and its mixing coefficient in the moving GMM along the control and the state. The function Ψ maps the displacement to a cost value, e.g., $\sum_{\mathbf{e}_i \in \mathbf{e}} |\mathbf{e}_i|$, where $|\cdot|$ is the defined as an L^2 -norm.



The dynamics in Eq. (10b) is a 2D single integrator system, which mimics the behaviour of a real UAV in our experimental setup to a reasonable extent (see Sec. IV).

The problem is formulated to find the optimal control, displacement, and probability for each Gaussian, ensuring that the displacement and probability deviate minimally from the ideal case, n.b., here the Gaussians represent the history of the explored space. For practical purposes, a given horizon $N \in \mathbb{N}_{>0}$ is defined, and the optimization is reiterated for each horizon using a methodology similar to an MPC controller, i.e., \mathcal{T} in Eq. (4) is the interval in between t and $t - N$.

The large-scale exploration is considered concluded when a desired level of coverage is achieved (see Sec. IV). It is also possible to set up the problem so that the exploration does not terminate or lasts for long-term, such as in [28].

Other practical considerations, such as the choice of the history and the size of the moving GMM, are detailed in the next section.

IV. EXPERIMENTAL RESULTS

This section provides an overview of our experimental setup and showcases the results. Simulated experiments are implemented utilizing MATLAB (R), whereas physical experimental setup is aided with a routine that utilizes Python and conducted with the popular DJI (R) Mavic 3 Classic Unmanned Aerial Vehicle (UAV). The exploratory trajectories are imported into the UAV’s flight controller utilizing waypoints, which is handled by a proprietary software component; but portability with other software components and flight controllers is supported (see Sec. V). The MPC optimization stack, i.e., the solver that solves the OCP in Eq. (10), relies on two external open-source components. The non-linear programming solver IPOPT [29] and the algorithmic differentiation library CasADi [30].

In the following, Sec. IV-A describes simulated experimental results, a forest with an area of 3 600 squared meters. Sec. IV-B details our finding in terms of built-in obstacle avoidance capabilities against coverage of our general scaled

ergodic controller. Sec. IV-C describes our real-world experimental results, a vegetated area with multiple obstacles with a total area of 10 000 squared meters.

A. Simulated forest

Simulated results are conducted in a forest with 45 trees spread randomly in area of 3 600 squared meters. The history h is set to 100 time steps (see Sec. IV-B). The simulation is terminated at 10 000 time step, when a desired coverage threshold is achieved within a certain approximation (i.e., 60% \pm 5%). The number of Gaussians n is set to five, whereas the initial position is set to the middle of the state space. The number of frequencies κ is set to nine, excluding the base frequency, which in line with other ergodic controllers in the literature [28].

Fig. 2 shows the results for the simulated forest at tree distinct time steps. Fig. 2a shows the trajectory (right of the figure) after 1 000 time steps. The history is illustrated with the dark-red line and the current point with the dark-red dot. The top-left of the figure shows the underlying information density distribution (i.e., the moving GMM in Definition II.2) with a detail of the five Gaussian components in the area that represents the current history interval. The optimal value of the Gaussians centers μ and of the mixing coefficients α are such that the moving GMM represents the history (i.e., the expected value and the covariance of the trajectory on the current history window) and that the Gaussians are deviated as little as possible to avoid the obstacles. The bottom-left of the figure shows the coverage map, where each square counts the number of points in within the square in a given time.

Fig. 2b shows the trajectory at time instant 2 500. The simulated UAV keeps flying through the obstacles, exploring further the state space. The moving GMM is then shown on the top-right, whereas the coverage map is shown at the bottom-right.

Fig. 2c shows the trajectory at time instant 10 000. Similarly to the previous figures, the moving GMM model and the coverage are illustrated at the top-left and bottom-left respectively. One can notice that while the obstacles are overall avoided, the simulated UAV come close or even passes through the obstacles at times. We report a relation in between the degree of obstacle avoidance capabilities and the coverage, as discussed in the next section.

B. Obstacle avoidance vs. coverage

The OCP posed as Eq. (10) might, at times, find no optimal solutions. In this scenario, our algorithm is such that a sub-optimal solution is returned, where the constraint expressed in Eq. (??) is not respected, e.g., the simulated trees in Sec. IV-A are not avoided with the desired threshold.

C. Real-world experiments

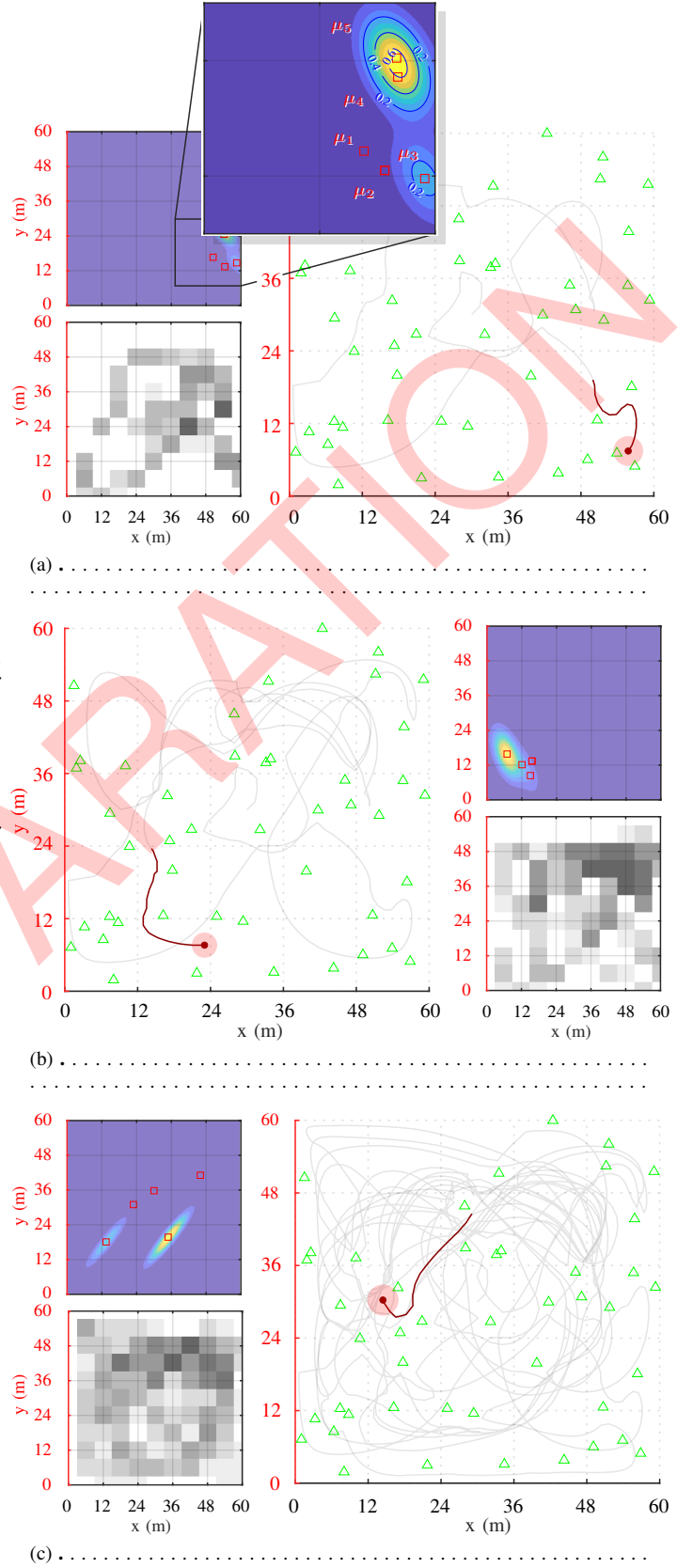


Fig. 2:

V. CONCLUSION AND FUTURE DIRECTIONS

REFERENCES

- [1] M. Popović, T. Vidal-Calleja, G. Hitz, J. J. Chung *et al.*, “An informative path planning framework for UAV-based terrain monitoring,” *Autonomous Robots*, vol. 44, no. 6, pp. 889–911, 2020. [1](#)
- [2] L. Schmid, M. Pantic, R. Khanna, L. Ott *et al.*, “An efficient sampling-based method for online informative path planning in unknown environments,” *IEEE Robotics and Automation Letters*, vol. 5, no. 2, pp. 1500–1507, 2020. [1](#)
- [3] L. M. Miller, Y. Silverman, M. A. MacIver, and T. D. Murphey, “Ergodic exploration of distributed information,” *IEEE Transactions on Robotics*, vol. 32, no. 1, pp. 36–52, 2016. [1](#)
- [4] G. Mathew and I. Mezić, “Metrics for ergodicity and design of ergodic dynamics for multi-agent systems,” *Physica D: Nonlinear Phenomena*, vol. 240, no. 4, pp. 432–442, 2011. [1](#), [2](#)
- [5] I. Abraham, A. Prabhakar, M. J. Z. Hartmann, and T. D. Murphey, “Ergodic exploration using binary sensing for nonparametric shape estimation,” *IEEE Robotics and Automation Letters*, vol. 2, no. 2, pp. 827–834, 2017. [1](#), [2](#)
- [6] L. M. Miller and T. D. Murphey, “Trajectory optimization for continuous ergodic exploration,” in *IEEE American Control Conference (ACC)*, 2013, pp. 4196–4201. [1](#), [2](#)
- [7] C. Lerch, D. Dong, and I. Abraham, “Safety-critical ergodic exploration in cluttered environments via control barrier functions,” in *IEEE International Conference on Robotics and Automation (ICRA)*, 2023, pp. 10 205–10 211. [1](#), [2](#), [3](#)
- [8] A. Prabhakar, I. Abraham, A. Taylor, M. Schlafly *et al.*, “Ergodic specifications for flexible swarm control: From user commands to persistent adaptation,” in *Conference on Robotics: Science and Systems (RSS)*, 2020, p. 9. [1](#)
- [9] D. Dong, H. Berger, and I. Abraham, “Time optimal ergodic search,” in *Conference on Robotics: Science and Systems (RSS)*, 2023, p. 13. [1](#), [2](#)
- [10] A. Seewald, C. J. Lerch, M. Chancán, A. M. Dollar *et al.*, “Energy-aware ergodic search: Continuous exploration for multi-agent systems with battery constraints,” in *IEEE International Conference on Robotics and Automation (ICRA)*, 2024, pp. 7048–7054. [1](#), [2](#)
- [11] K. B. Naveed, D. Agrawal, C. Vermillion, and D. Panagou, “Eclares: Energy-aware clarity-driven ergodic search,” in *IEEE International Conference on Robotics and Automation (ICRA)*, 2024, pp. 14 326–14 332. [1](#)
- [12] I. Abraham, A. Prabhakar, and T. D. Murphey, “An ergodic measure for active learning from equilibrium,” *IEEE Transactions on Automation Science and Engineering*, vol. 18, no. 3, pp. 917–931, 2021. [1](#), [2](#)
- [13] Z. Ren, A. K. Srinivasan, B. Vundurthy, I. Abraham *et al.*, “A pareto-optimal local optimization framework for multiobjective ergodic search,” *IEEE Transactions on Robotics*, pp. 1–12, 2023. [1](#)
- [14] A. K. Srinivasan, G. Gutow, Z. Ren, I. Abraham *et al.*, “Multi-agent multi-objective ergodic search using branch and bound,” in *IEEE/RSJ International Conference on Intelligent Robots and Systems (IROS)*, 2023, pp. 844–849. [1](#)
- [15] S. Shetty, J. Silvério, and S. Calinon, “Ergodic exploration using tensor train: Applications in insertion tasks,” *IEEE Transactions on Robotics*, vol. 38, no. 2, pp. 906–921, 2022. [1](#)
- [16] C. Bilaloglu, T. Löw, and S. Calinon, “Whole-body ergodic exploration with a manipulator using diffusion,” *IEEE Robotics and Automation Letters*, vol. 8, no. 12, pp. 8581–8587, 2023. [1](#)
- [17] T. Löw, J. Maceiras, and S. Calinon, “drosBot: Using ergodic control to draw portraits,” *IEEE Robotics and Automation Letters*, vol. 7, no. 4, pp. 11 728–11 734, 2022. [1](#)
- [18] A. Prabhakar, A. Mavrommati, J. Schultz, and T. D. Murphey, “Autonomous visual rendering using physical motion,” in *Workshop on the Algorithmic Foundations of Robotics (WAFR)*. Springer, 2020, pp. 80–95. [1](#)
- [19] G. De La Torre, K. Flaßkamp, A. Prabhakar, and T. D. Murphey, “Ergodic exploration with stochastic sensor dynamics,” in *IEEE American Control Conference (ACC)*, 2016, pp. 2971–2976. [1](#)
- [20] E. Ayvali, H. Salman, and H. Choset, “Ergodic coverage in constrained environments using stochastic trajectory optimization,” in *IEEE/RSJ International Conference on Intelligent Robots and Systems (IROS)*, 2017, pp. 5204–5210. [1](#)
- [21] A. Rao, G. Sartoretti, and H. Choset, “Learning heterogeneous multi-agent allocations for ergodic search,” in *IEEE International Conference on Robotics and Automation (ICRA)*, 2024, pp. 12 345–12 352. [1](#)
- [22] H. Coffin, I. Abraham, G. Sartoretti, T. Dillstrom *et al.*, “Multi-agent dynamic ergodic search with low-information sensors,” in *IEEE International Conference on Robotics and Automation (ICRA)*, 2022, pp. 11 480–11 486. [1](#)
- [23] L. Dressel and M. J. Kochenderfer, “On the optimality of ergodic trajectories for information gathering tasks,” in *IEEE American Control Conference (ACC)*, 2018, pp. 1855–1861. [1](#)
- [24] A. Rao, A. Breiffeld, A. Candela, B. Jensen *et al.*, “Multi-objective ergodic search for dynamic information maps,” in *IEEE International Conference on Robotics and Automation (ICRA)*, 2023, pp. 10 197–10 204. [1](#)
- [25] E. Wittemyer and I. Abraham, “Bi-level image-guided ergodic exploration with applications to planetary rovers,” in *IEEE/RSJ International Conference on Intelligent Robots and Systems (IROS)*, 2023, pp. 10 742–10 748. [1](#)
- [26] I. Abraham and T. D. Murphey, “Decentralized ergodic control: Distribution-driven sensing and exploration for multiagent systems,” *IEEE Robotics and Automation Letters*, vol. 3, no. 4, pp. 2987–2994, 2018. [2](#)
- [27] S. Calinon, *Mixture models for the analysis, edition, and synthesis of continuous time series*. Springer, 2020, pp. 39–57. [3](#)
- [28] A. Seewald, H. García de Marina, H. S. Midtiby, and U. P. Schultz, “Energy-aware planning-scheduling for autonomous aerial robots,” in *IEEE/RSJ International Conference on Intelligent Robots and Systems (IROS)*, 2022, pp. 2946–2953. [3](#), [4](#)
- [29] A. Wächter and L. T. Biegler, “On the implementation of an interior-point filter line-search algorithm for large-scale nonlinear programming,” *Mathematical Programming*, vol. 106, no. 1, pp. 25–57, 2006. [3](#)
- [30] J. Andersson, J. Åkesson, and M. Diehl, “CasADi: A symbolic package for automatic differentiation and optimal control,” in *Conference on Recent Advances in Algorithmic Differentiation (AD)*. Springer, 2012, pp. 297–307. [3](#)